air, and, less frequently, very moist tropic air from the vicinity of Hawaii (*12*). Once every few years, an invasion of Arctic air from interior Alaska or the Yukon occurs, bringing record cold temperatures. The long-term decrease in the δD values of the precipitations may be a result of changes in proportions of warm versus cold precipitation (for example, summer versus winter precipitation). It is also possible that variations reflect an increase in the frequency of the extremely cold events or a decrease in the frequency of the warm events. This set of observations may, therefore, provide valuable data for the validation of climatic simulations concerning changes in atmospheric circulation patterns.

REFERENCES AND NOTES

1. W. S. B. Paterson *et al.*, *Nature* **266**, 508 (1977).
2. W. Dansgaard, S. J. Johnsen, H. B. Clausen, C. C. Langway, in *The Late Cenozoic Glacial Ages*, K. K. Truekian, Ed. (Yale Univ. Press, New Haven, CT, 1971), pp. 37–56; S. J. Johnsen, W. Dansgaard, H. B. Clausen, C. C. Langway, *Nature* **235**, 429 (1972); *ibid.* **236**, 249 (1972); P. M. Grootes, M. Stuiver, J. W. C. White, S. Johnsen, J. Jouzel, *ibid.* **366**, 552 (1993).
3. COHMAP Members, *Science* **241**, 1043 (1988).
4. V. C. LaMarche Jr., *Quat. Res.* **3**, 632 (1993).
5. B. H. Luckman, *Can. J. Earth Sci.* **25**, 148 (1988).
6. The δD and $\delta^{18}O$ are defined as

$$\delta D = \left[\frac{(D/H)_{sample}}{(D/H)_{standard}} - 1\right] \times 1000$$

and

$$\delta^{18}O = \left[\frac{(^{18}O/^{16}O)_{sample}}{(^{18}O/^{16}O)_{standard}} - 1\right] \times 1000$$

where standard is standard mean ocean water (SMOW).
7. S. Epstein and C. Yapp, *Nature* **266**, 477 (1977).
8. J. W. White, J. R. Lawrence, W. S. Broecker, *Geochim. Cosmochim. Acta* **58**, 851 (1994).
9. S. Epstein and C. J. Yapp, *Earth Planet. Sci. Lett.* **30**, 252 (1976); C. J. Yapp and S. Epstein, *ibid.* **34**, 333 (1977).
10. C. J. Yapp and S. Epstein, *Nature* **297**, 636 (1982).
11. T. W. D. Edwards and P. Fritz, *Appl. Geochem.* **1**, 715 (1986); S. Epstein and R. V. Krishnamurthy, *Philos. Trans. R. Soc. London Ser. A* **330**, 427 (1990).
12. C. A. Hall Jr., D. L. Elliott-Fisk, A. M. Peterson, D. R. Powell, H. E. Kleiforth, in *Natural History of the White-Inyo Range*, C. A. Hall, Ed. (Univ. of California Press, 1991), pp. xv, 6–7, and 91.
13. S. Epstein, C. J. Yapp, J. Hall, *Earth Planet. Sci. Lett.* **30**, 241 (1976); M. J. DeNiro, *ibid.* **54**, 177 (1981).
14. R. Ramesh, S. K. Bhattacharya, K. Gopalan, *Nature* **317**, 802 (1985).
15. X. Feng, C. J. Yapp, S. Epstein, unpublished data.
16. J. E. Kutzback and P. J. Guetter, *J. Atmos. Sci.* **43**, 1726 (1986).

17. Supported by NSF grant ATM9219891 and by the U.S. Department of Energy under Cooperative Agreement Award DE-FC03-90ER61010. The samples were provided by M. Hughes at the Tree Ring Laboratory, University of Arizona, Tucson, Arizona. We also thank D. A. Graybill, E. Dent, and X. Xu for technical support.

22 March 1994; accepted 29 June 1994

Stream Networks and Long-Term Surface Uplift in the New Madrid Seismic Zone

Dorothy Merritts and Tim Hesterberg

Stream networks are sensitive to low rates of surface uplift and can be used to decipher the history of large earthquakes even where faults do not rupture the surface, as in intraplate seismic zones. Statistical analysis of alluvial network data from topographic maps in the New Madrid seismic zone, in the central United States, shows that stream-segment gradients deviate the most from an estimated natural stream profile where surface uplift is greatest. Evidence of cumulative deformation distilled from stream network patterns represents at least several meters of differential surface uplift during Holocene time, which suggests that more than one cycle of surface deformation occurred.

Landform geometry reflects crustal tectonics, and geomorphic features provide a bridge between deformation on the time scales of several earthquake cycles (10^2 to 10^4 years) and recent geodetic surveys (1 to 100 years). Landforms generally analyzed include fault-bounded mountain fronts, offset stream channels, or uplifted coastlines along active plate margins and in deforming mountain belts where faults commonly break the surface. Using landforms to extend prehistoric seismic records in continental interiors where earthquakes are common (*1*) has been unsuccessful because faults rarely rupture the surface in continental interiors and the terrain in such areas typically has little relief. Here, elevation changes in 15 stream networks were analyzed for deformation resulting from the succession of large earthquakes in 1811 and 1812 in New Madrid, Missouri, a continental interior location with historic earthquake activity (*1*).

The New Madrid seismic zone (NMSZ) spans Quaternary deposits on the borders of Kentucky, Missouri, Arkansas, and Tennessee. More than 1 km of alluvial sediment mantles the continental crust and obscures crustal displacement (*2*). In 1811 and 1812, the three largest earthquakes (magnitude ~8.1 to 8.3) known to have occurred in the continental North American plate emanated near New Madrid (*1*). Although this region is far from a plate boundary, it has had nearly continuous microearthquake activity throughout monitoring in this century (*3*). Shear strain rates are as much as one-third of those along faults forming active plate margins, such as the San Andreas (*4*). Geodetic and geomorphic evidence indicates that tilting is occurring in the mid-continent and might be the cause of downstream changes in channel sinuosity along large rivers (*5, 6*), and paleoseismic investigations of liquefied sands indicate that large earthquakes might have occurred many times during the past several thousand years (*7–9*). Some of the aerially extensive, low-relief features within the NMSZ, such as the Lake County uplift, are related to both active faults and historic seismicity (*8, 10–12*). Other such features either are not or their relation to underlying geologic structures is not yet known (*13–15*).

We studied the Lake County uplift (LCU) region where substantial surface deformation is known to occur and its pattern is clearly established. The LCU is a gourd-shaped, composite Quaternary structure containing anomalous relief (Fig. 1A), active faults, and much seismic activity (*10, 11*). The area of the LCU is about 50 by 23 km and upwarps the Mississippi River valley as much as 10 m. Seismic reflection data indicate that subsurface rocks are upwarped in a manner that parallels the pattern of surface warping (*10, 11*). Seventy-five percent of microearthquakes recorded in the NMSZ between July 1974 and June 1978 occurred within the LCU.

From analysis of warped, active as well as abandoned channels and levees of the Mississippi River, Russ (*10*) divided the LCU into three prominent topographic bulges: Tiptonville Dome, Ridgeley Ridge, and Sikeston Ridge (Fig. 1A) (*10*). We focused on the area encompassed by Tiptonville Dome and Ridgeley Ridge, including their perimeters where Russ's (*10*) estimate of surface uplift tapers to 0. Most of the Tiptonville Dome formed between 200 and 2000 years ago, but additional uplift occurred during the 1811 and 1812 New Madrid earthquakes (*10, 11*). Russ (*10*) estimated that up to 9 to 10 m of surface uplift has occurred, which indicates that rates of surface uplift (4 to 5 mm $year^{-1}$) are as high as those along active plate margins dominated by compression (*16*). Ridgeley Ridge, formed <6000 years ago, is underlain by northeast-trending faults, some of which are possibly high-angle reverse faults, and its surface expression mimics the subsurface structural pattern (*10, 11*).

The northeastern boundary of the LCU

D. Merritts, Department of Geosciences, Franklin & Marshall College, Lancaster, PA 17604, USA.
T. Hesterberg, Department of Mathematics, Franklin & Marshall College, Lancaster, PA 17604, USA.

is probably a southwest-dipping (31°), northwest-striking reverse fault (*17*), forming a contractional step-over between near-vertical, right-lateral northeast-trending faults of the NMSZ. The LCU is located in the overriding hanging wall block and is rising relative to the footwall block to its north, which contains a lake created during the 1811 and 1812 earthquakes (*18*). Using these probable fault geometries and three-dimensional boundary-element modeling, Gomberg and Ellis (*19*) identified a pattern of deformation very similar to that determined by Russ (*10*).

In contrast to these results (*10*, *19*) our deformation estimates are based on stream gradient data from U.S. Geological Survey topographic maps (Fig. 2) and extend previously described methodology (*16*). Stream channels have natural gradients that depend primarily on resistance to flow (which is dependent on bedrock or sediment type and properties) and volume of water and sediment flowing in the stream (*20*, *21*). If tectonic processes elevate the upstream end of a segment a different amount than the downstream end, the stream will attempt to return to its natural gradient by incising, aggrading, or altering its sinuosity (*22–24*). We hypothesize that landscaping processes in the NMSZ have not completed this incision or aggradation, so that a record of deformation is preserved in the channel gradients. Thus, streams flowing in the direction the surface was tilted will be relatively steep, whereas streams flowing in the opposite direction will be relatively gentle (*25*).

We used digitized topographic data for 15 small streams that drain the LCU (drainage areas <30 km^2) because their gradients and orientations are sensitive to surface deformation (*16*) and because they are not as likely as larger streams to erase evidence of perturbations. We delineated all stream segments in the region (Figs. 1B and 2) on large-scale maps (1:24,000), not using stream segments altered by human activities (such as irrigation ditches). Data collection software digitized stream networks and calculated stream gradient and total upstream channel length for each segment (*26*).

We assumed that flow resistance is similar across the study area because all watersheds examined were developed in unconsolidated alluvium deposited by the Mississippi River in its floodplain or in loess blown in by glacial winds during the past several million years. We also assumed that the total length of all stream segments upstream of any given point is a proxy variable for flow volume (discharge) at that point, which has been shown to be valid (*27*). We assumed that discharge is a smooth increasing function of (but not necessarily proportional to) the total length of all upstream stream segments (*28*). If these assumptions hold, then the natural gradient of a stream depends solely on the total length of segments upstream of any point.

Our statistical model for estimating uplift from the elevation change (drop) between upstream and downstream ends of a stream segment is of the form

$$drop = f(l_2) - f(l_1) + g(x_1, y_1) - g(x_2, y_2) + \varepsilon \qquad (1)$$

where l_1 is the length of all stream segments

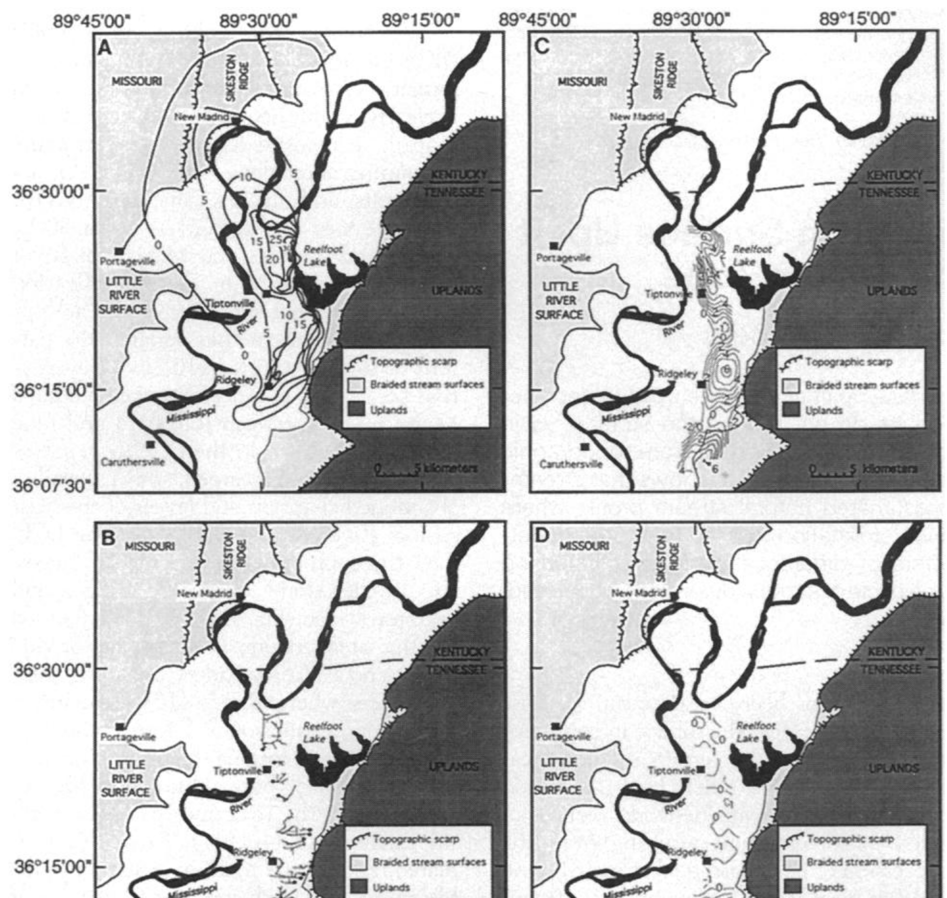

Fig. 1. Map of Lake County uplift region. (**A**) Surface uplift contours (feet) as obtained from Russ (*10*). (**B**) Watersheds analyzed in this study. The map simplifies the networks, in that only the endpoints of each stream segment, and a straight line between them, are shown. The mouth of each stream network is shown with a black dot. (**C**) Contours of uplift estimate *g* (in feet). (**D**) Contours of uplift estimate from one random (bootstrap) sample (in feet). The magnitudes of this and almost all other random uplift estimates are smaller than the magnitude of *g* because of the lack of a pattern in the random deviations of stream segment drops.

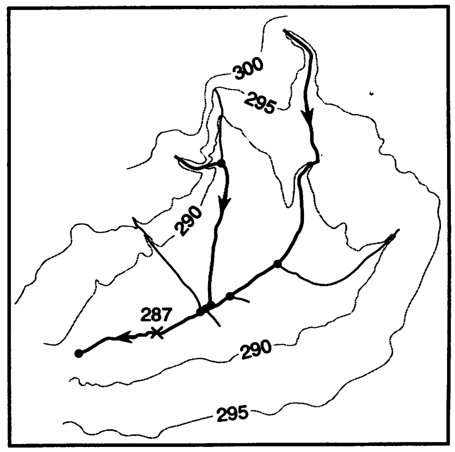

Fig. 2. Example of method used to delineate stream networks, using one of the watersheds from the LCU region (figure simplified from a 7.5-minute topographic map; 1:24,000 scale). Shaded thin lines correspond to elevation contours, in feet. Thick lines correspond to streams shown on the topographic maps as blue lines. Thin lines are segments added here to include all concavities in the landscape for which the contour "v" angle is less than 120°. This morphometric technique allowed us to identify areas where water is likely to collect, flow, and sculpt the landscape but that did not meet the criteria for channelized water used by cartographers. Black dots identify intersections between segments and mark segment endpoints. The "x" indicates the location of the benchmark.

upstream of the segment, $l_2 = l_1 +$ the length of the segment, (x_1, y_1) are coordinates of the upstream end of the segment, (x_2, y_2) are coordinates of the downstream end of the segment, f is a smooth increasing function that gives the natural profile of a stream, g is a smooth function that measures relative uplift, and ε is a combination of measurement error and randomness.

The streams are steep near the headwaters (Figs. 3 and 4), but within 1 km downstream the estimated gradient decreases to about 0.34 m km^{-1}, then gradually to 0.27 m km^{-1} after 10 km, and finally to 0.14 m km^{-1} after 40 km. The estimate of f was semiparametric because the data determined the shape of the profile; in comparison, others have used a parametric model of the form $f(x) = a \ln(x)$ (*24*). Our estimate of f used regression splines (*29*) of the form

$$f(x) = \sum_{i=1}^{4} a_i f_i(x^{0.28}) \qquad (2)$$

where values for f_i are piecewise cubic polynomials that are natural cubic splines (*30*).

The estimate of uplift g (Fig. 1C) is also semiparametric and used tensor regression splines, with coefficients penalized for numerical stability and to produce smoother functions. The amount of penalty is a smoothing parameter that can be controlled by the modeler to produce flatter and smoother profiles at one extreme or unflattened but jagged and unstable profiles at the other.

From contouring of the estimate of surface uplift g (Fig. 1C), uplift is generally greatest along the middle (from east to west) of the LCU study area, with low areas about one-quarter and one-half the distance from the south to the north. The pattern exhibits three elongate (in the north-south direction) bulges and one smaller, more circular bulge at the northernmost end of the LCU. However, fine details might result from the inherent randomness in stream channel elevations or the methodological limitations of working with elevation data from maps with 5-foot contour intervals in a region of very little relief. The contours are less accurate on the edges of the study area (a common problem in interpolation, regression, and contouring techniques), and because of smoothing the actual uplift is probably greater than indicated by g.

A bootstrap analysis (*31*) indicates that the overall uplift pattern is statistically significant. However, it is based solely on numerical criteria and cannot distinguish between true surface uplift and other spatial effects. For example, if streams flowing north tend to be steeper because sediment types on north-facing slopes are different than those on south-facing slopes, the model (Eq. 1) would indicate more uplift to the south, and the bootstrap analysis would tend to indicate that the result is statistically significant. Although such a change in sediment type could lead to a statistically significant pattern, purely random effects would be unlikely to produce such a strong consistent pattern as in Fig. 1C (see Fig. 1D).

Three reasonable causes of the statistically significant, organized change in channel gradient along the length of the LCU are (i) differences in local climate (and hence streamflow characteristics), (ii) spatial variations in underlying geologic material, or (iii) surface deformation attributable to tectonic activity. Local climatic differences are not likely, because the NMSZ is located in a continental interior and has little relief (<20 to 40 m). As a consequence, climatic conditions are remarkably uniform throughout its extent. Although we cannot rule out difference in resistance of underlying material, a tectonic cause is more likely. Low-order streams in the region are developed on a similar stratigraphic section of unconsolidated deposits that consists of Eocene deltaic and near-shore marine sediments overlain by Pliocene-Pleistocene river gravels, sands, and clay, which in turn are overlain locally by up to several tens of meters of fine, glacial loess (*32, 33*). The Quaternary-Eocene unconformity is at a depth of 50 to 100 m in most places. As topographic relief is so small, streams are incised into only the uppermost parts of this stratigraphic section. A blanket of unconsolidated, late Cenozoic alluvium is not likely to result in notable spatial differences in resistance to flow that in turn would cause such marked variations in channel bed elevations.

Clearly, stream channels are sensitive to surface uplift, and using differences in elevation drops in the LCU region results in an uplift pattern (Fig. 1C) that is similar to Russ's interpretation (*10*) of the best available physical evidence of surface uplift (Fig. 1A). Three of the four bulges in Fig. 1C are coincident with two areas of high surface uplift identified by Russ (*10*) (Fig. 1A), the Tiptonville Dome and Ridgeley Ridge. Compared to the use of channels and levees of large rivers to obtain a differential uplift pattern, this method gives a greater number and aerial extent of control points because the data are taken from all parts of the watersheds of small streams, which form a fairly dense network across the LCU area. These two patterns are also quite similar to that generated from three-dimensional boundary element modeling of the local deformation field that would result from a contractional left step-over along a northeast-trending right-lateral strike-slip fault [see figures 4 and 5 in (*19*)].

Analysis of channel gradients of low-order streams with statistical modeling identifies areas of surface deformation and offers a level of detail greater than that available from other methods. The fact that channel networks in the NMSZ reflect at least several meters of differential surface uplift (Fig. 1C) indicates that cumulative deformation spanning more than one earthquake cycle probably has occurred. If uplift in the region is largely coseismic, events like those of 1811 and 1812 might have

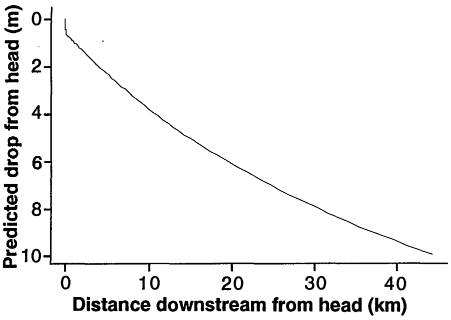

Fig. 3. Estimated natural stream profile form for the New Madrid seismic zone.

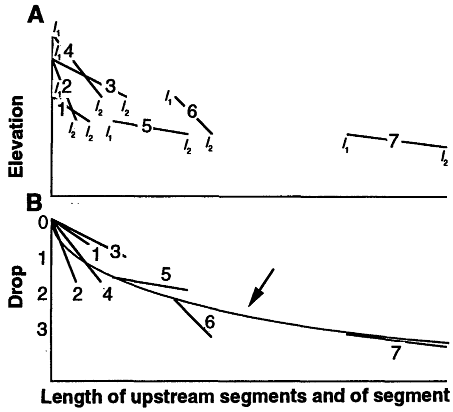

Fig. 4. Schematic diagram of the natural profile model of Fig. 3. (**A**) A simple seven-segment basin, with each stream segment shown as a straight line. The position of each segment is relative to its upstream and downstream endpoint elevations and upstream-contributing stream length. Feeder segments numbered 1 and 2 flow into segment 5; feeder segments 3 and 4 flow into segment 6; and segments 5 and 6 likewise flow into segment 7. The end elevation of each feeder segment matches the beginning elevation for the segment into which it flows, and the value of l_1 for the downstream segment is the sum of the lengths for all the feeder segments. (**B**) The same stream segments as (A), moved so that the upstream endpoint is located on the curve marked with an arrow, the estimate of natural profile f. Segments 1, 3, and 5 drop less than predicted by the profile (based on their lengths and the lengths of upstream segments), and segments 2, 4, 6, and 7 drop more than predicted. Such deviations might be due to differential uplift throughout the study area.

occurred before, in the geologically recent past (34). Gomberg and Ellis (19) assumed that events like those of 1811 and 1812 occur about every 1000 years and estimated about 15 to 60 cm of surface uplift per 1000 years (including coseismic uplift and post-seismic relaxation). Our results indicate that the LCU block has been rising relative to the Reelfoot Lake block long enough to affect the gradients of some parts of stream networks in the region by at least several meters. Furthermore, as these streams drain recent deposits, uplift has occurred since the time of deposition of the youngest sediments (mid to late Holocene). If each cycle of deformation results in less than 1 m of net uplift, the results of the stream-gradient analysis indicate that more than one cycle has occurred during Holocene time. This also provides evidence that low-order streams adjust their gradients slowly enough for uplift patterns to persist in the landscape record over several thousand years.

REFERENCES AND NOTES

1. M. L. Fuller, *U.S. Geol. Surv. Bull.* **494**, 119 (1912); O. W. Nuttli, *Bull. Seismol. Soc. Am.* **63**, 227 (1973); A. C. Johnston and S. J. Nava, *J. Geophys. Res.* **90**, 6737 (1985); A. C. Johnston and L. R. Kanter, *Sci. Am.* **262**, 68 (1990).
2. F. A. McKeown, *U.S. Geol. Surv. Prof. Pap. 1236* (1982), p. 1.
3. W. Stauder, *ibid.*, p. 21.
4. L. Liu, M. D. Zoback, P. Segall, *Science* **257**, 1666 (1992).
5. J. Adams, *Geology* **8**, 442 (1980).
6. A. W. Burnett and S. A. Schumm, *Science* **222**, 49 (1983).
7. R. T. Saucier, *Geology* **19**, 296 (1991).
8. K. I. Kelson, R. B. VanArsdale, G. D. Simpson, W. R. Lettis, *Seismol. Res. Lett.* **63**, 349 (1992).
9. J. D. Vaughn, *U.S. Geol. Surv. Open-File Rep. 93-195* (1993), p. 95.
10. D. P. Russ, *U.S. Geol. Surv. Prof. Pap. 1236*, p. 95.
11. R. L. Wheeler and S. Rhea, *U.S. Geol. Surv. Misc. Field Stud. Map 2264-E, Scale 1:250,000 (1994).*
12. D. P. Russ, *Geol. Soc. Am. Bull.* **90**, 1013 (1979).
13. R. B. VanArsdale *et al.*, *Seismol. Res. Lett.* **63**, 309 (1992).
14. R. T. Cox, *Southeast. Geol.* **28**, 211 (1988).
15. K. D. Nelson and J. Zhang, *Tectonophysics* **197**, 271 (1991).
16. D. Merritts and K. R. Vincent, *Geol. Soc. Am. Bull.* **101**, 1373 (1989).
17. J. M. Chiu, A. C. Johnston, Y. T. Yang, *Seismol. Res. Lett.* **63**, 375 (1992).
18. D. W. Stahle, R. B. VanArsdale, M. K. Cleaveland, *ibid.*, p. 439.
19. J. Gomberg and M. Ellis, *J. Geophys. Res.*, in press.
20. S. A. Schumm, *The Fluvial System* (Wiley, New York, 1977).
21. ———, in *Active Tectonics* (National Academy of Sciences Press, Washington, DC, 1983), pp. 80–94.
22. Z. B. Begin, D. F. Meyer, S. A. Schumm, *Earth Surf. Processes Landforms* **6**, 49 (1981).
23. S. Ouchi, *Geol. Soc. Am. Bull.* **96**, 504 (1985).
24. R. S. Snow and R. L. Slingerland, *J. Geol.* **95**, 15 (1987).
25. This hypothesis was tested and confirmed in coastal northern California, at the northern termination of the San Andreas fault, where uplift rates range from low (<0.4 mm year^{-1}) to high (3 to 4 mm year^{-1}) and streams are incising sedimentary bedrock (16).
26. The manual data extraction techniques of Merritts and Vincent (16) were updated with new software. Furthermore, the multivariate statistical analysis has been replaced with a much more flexible and powerful method of analysis that uses S-Plus language, a high-level statistical programming environment [R. A. Becker, J. M. Chambers, A. R. Wilks, *The New S Language* (Wadsworth and Brooks/Cole, Pacific Grove, CA, 1988); *S-PLUS Reference Manual, Version 3.0* (Statistical Sciences, Seattle, WA, 1991); J. M. Chambers and T. J. Hastie, *Statistical Models in S* (Wadsworth and Brooks/Cole, Pacific Grove, CA, 1992)]. Data collection software works with Macintosh hardware and an Altek AC-40 digitizer; the resolution of the digitizer is 0.001 inches, or 2 feet at the map scale. We constructed a database for all 15 stream segments in the LCU region. The database includes elevations (starting and ending points), lengths, gradients, coordinate positions of upstream and downstream ends of stream segments, and weighted average azimuth orientations for each stream segment.
27. J. T. Hack, *U.S. Geol. Surv. J. Res.* **1**, 421 (1973).
28. An alternative way to model discharge from topographic data would be to assume that it is proportional to drainage area, but this would require delineating and measuring stream drainage areas (rather than lengths) upstream of all segment intersections.
29. T. J. Hastie and R. J. Tibshirani, *Generalized Additive Models* (Chapman & Hall, New York, 1990).
30. The exponent 0.28 in Eq. 2 was chosen from a parametric model predicting uplift solely as a function of I_1 and I_2. The f and g functions are estimated simultaneously, and the g estimate is relatively insensitive to changes in the exponent in Eq. 2, with a correlation of 0.991 between uplift estimates resulting from the exponents of 0.28 and 1.0.
31. B. Efron and R. J. Tibshirani, *An Introduction to the Bootstrap* (Chapman & Hall, New York, 1993).
32. R. T. Saucier, *U.S. Army Corps of Engineers, Waterways Experiment Station Technical Report 3-659* (1964).
33. ———, *Ark. Archeol. Surv. Res. Ser.* **6**, 26 (1974).
34. A. C. Johnston and K. M. Shedlock, *Seismol. Res. Lett.* **63**, 193 (1992).

35. We thank T. Hastie for regression splines for estimating the natural profile of streams; H. Haddon for developing the Digistream software; D. Muriceak for collecting the data; and several geologists with expertise in the New Madrid seismic zone for advice, suggestions, and information, including R. Wheeler, E. Schweig, M. Ellis, P. Bodin, and A. Crone. Supported by the U.S. Geological Survey (USGS) under USGS award number 1408-93-G-2230.

25 February 1994; accepted 7 June 1994

Virulence and Local Adaptation of a Horizontally Transmitted Parasite

Dieter Ebert*

Parasites are thought to maximize the number of successfully transmitted offspring by trading off propagule production against host survival. In a horizontally transmitted microparasitic disease in *Daphnia*, a planktonic crustacean, increasing geographic distance between host and parasite origin was found to be correlated with a decrease in spore production and virulence. This finding indicates local adaptation of the parasite, but contradicts the hypothesis that long-standing coevolved parasites are less virulent than novel parasites. Virulence can be explained as the consequence of balancing the positive genetic correlation between host mortality and strain-specific spore production.

Parasites are considered to be a major factor influencing almost every level of organismic evolution (1, 2). Conventional wisdom holds that successful parasite species should evolve to become less virulent over time and therefore that only maladapted novel parasites are harmful (3). In contrast, current theory on the evolution of virulence states that pathogenicity can be maintained when it is a direct or indirect consequence of the parasite's exploitation of the host during production of propagules. Therefore, a horizontally transmitted parasite is expected to balance parasite reproduction against host survival, such that parasite transmission is maximized (4, 5).

To understand the processes that influence the evolution of virulence, I studied host fecundity and survival alongside parasite multiplication rate and infectivity in a laboratory transplant experiment. I used host clones of the planktonic crustacean *Daphnia magna* Straus derived from localities up to 3000 km apart and three strains of the horizontally transmitted, cytoplasmic parasite *Pleistophora intestinalis* Chatton [Protozoa, Microsporidia (6)] collected from three ponds near Oxford, United Kingdom (Table 1). Horizontal transmission of this parasite occurs when infected hosts pass infective spores with their feces and other hosts capture and ingest the free-floating spores by filter feeding. Vertical transmission does not occur in this microparasite (7). Sporeload, here defined as the number of sporophorous vesicles found within the host gut epithelium, increases exponentially over time, which allows estimation of parasite multiplication rate (7). The impact

Zoology Department, Oxford University, South Parks Road, Oxford OX1 3PS, UK.

*Present address: Centre for Population Biology, Imperial College at Silwood Park, Ascot, Berks SL5 7PY, UK.